Received: 13 October 2020 | Revised: 17 December 2020 | Accepted: 12 January 2021

DOI: 10.1002/ptr.7030

RESEARCH ARTICLE

WILEY

Oroxylin A is a severe acute respiratory syndrome coronavirus 2-spiked pseudotyped virus blocker obtained from Radix Scutellariae using angiotensin-converting enzyme II/cell membrane chromatography

Jiapan Gao | Yuanyuan Ding | Yuejin Wang | Peida Liang | Liyang Zhang | Rui Liu

School of Pharmacy, Xi'an Jiaotong University, Xi'an, China

Correspondence
Rui Liu, School of Pharmacy, Xi'an Jiaotong University, Yanta West Road, Xi'an 710061, China.
Email: rliu2018@xjtu.edu.cn

Funding information
China Postdoctoral Science Foundation, Grant/Award Number: 2019M663755; National Natural Science Foundation of China, Grant/Award Numbers: 81930096, 81903572

The current worldwide outbreak of the coronavirus disease 2019 (COVID-19) has been declared a public health emergency. The angiotensin-converting enzyme II (ACE2) has been reported as the primary host-cell receptor for severe acute respiratory syndrome coronavirus 2 (SARS-CoV-2), the causative virus of COVID-19. In this study, we screened ACE2 ligands from Radix Scutellariae and investigated its suppressive effect on SARS-CoV-2 spiked pseudotyped virus in vitro. HEK293T cells stably expressing ACE2 receptors (ACE2 cells) were used to provide the receptor for the ACE2/cell membrane chromatography (CMC) method used for analysis. The SARS-CoV-2-spiked pseudotyped virus was used to examine the anti-viropexis effect of the screened compounds in ACE2 cells. Molecular docking and the surface plasmon resonance (SPR) assay were used to determine the binding properties. Oroxylin A exhibited an appreciable suppressive effect against the entrance of the SARS-CoV-2-spiked pseudotyped virus into ACE2 cells, which showed good binding to ACE2 as determined using SPR and CMC. Oroxylin A was shown to be a potential candidate in the treatment for COVID-19 by virtue of its blocking the entrance of SARS-CoV-2 into ACE2 cells by specifically binding to the ACE2 receptor.

KEYWORDS
ACE2, CMC, COVID-19, Oroxylin A, Radix Scutellariae

1 | INTRODUCTION

The coronavirus disease 2019 (COVID-19) has been rapidly spreading worldwide since December 2019 (Huang et al., 2020). The main symptoms of COVID-19 infection include fever, dry cough, fatigue, myalgia, and diarrhea and this condition could further lead to the severe respiratory syndrome, septic shock, and even death. Similar to other previous outbreaks of newly discovered viral infections, no conventional drugs have been proven to be effective treatment options. According to recent reports, the early use of lopinavir/ritonavir as a therapeutic drug in patients with severe acute respiratory syndrome (SARS) infections could reduce mortality and intubation rates (Jin et al., 2020).

Ribavirin has also been widely used for SARS based on its broad-spectrum antiviral activity. Studies of ribavirin combined with corticosteroids in the early SARS case series have shown that clinical improvement with this combination is still controversial (Lee et al., 2003; Ho et al., 2003). In addition, β-interferon, glucocorticoid, and supportive treatment with Remdesivir have been reported to be effective in the management of COVID-19 (Jin et al., 2020; Wang et al., 2020; Holshue et al., 2020).

Abbreviations: ACE2 cells, HEK293T cells stably expressing ACE2; ACE2, angiotensin-converting enzyme II; CCK-8, cell counting kit-8; CIB, calcium imaging buffer; CMC, cell membrane chromatography; TCM, traditional Chinese medicine.

In China, most therapies for this pandemic include traditional Chinese medicine (TCM) formulations. Recently, some published studies have shown that TCM preparations shortened the fever reduction time and the average length of hospital stay (Wang & Babina, 2020; Xiong, Wang, Su, Cho, & Xing, 2020; Zhong et al., 2020). TCM research has provided a promising new strategy for the clinical treatment of this scourge. Radix Scutellariae, known as Huang-Qin in China, has been used as Chinese herbal medicine for more than 2,000 years (Zhao, Chen, & Martin, 2016).

Scutellaria has been reported to be useful for treating ulcerative colitis (Liang et al., 2019), fibrosis, and lipid peroxidation in the liver (Wu, Zhi, Lun, Deng, & Zhang, 2018), and is also known to have antibacterial (Tsai et al., 2018) and antiviral (Kitamura et al., 1998) effects. Various natural products have been isolated from *Scutellaria* plants including amino acids, flavonoids, essential oils, phenylethanoids, and sterols. More than 30 types of flavones can be found in the roots including oroxylin A, baicalein, baicalin, chrysin, and wogonin (Li, Jiang, & Chen, 2004). However, no studies have reported the anti-COVID-19 activity of Radix Scutellariae or its mechanism of action.

Cell membrane chromatography (CMC) is a typical high-throughput bioaffinity method that has been used successfully in the screening of potent compounds from TCM preparations. For example, the anti-allergic component of Saposhnikoviae Radix extracts have been screened using mas-related gene X2 (MrgX2)/CMC (Jia et al., 2019) and the antitumor components of *Ligusticum wallichii* extracts were screened using fibroblast growth factor receptor 4 (FGFR4)/CMC (Zhang, Ding, An, Feng, & Wang, 2015).

In addition, Fructus Schisandrae Chinensis extracts were screened for anti-hypertensive components using isolated tissues such as the vascular smooth muscle (VSM)/CMC (Yang, Wang, Zhang, Chang, & Li, 2011). CMC can also be used to investigate the interaction between active compounds and specific receptors and to determine the equilibrium dissociation constant, K_D (Han et al., 2018; Lin, Lv, Fu, Jia, & Han, 2018; Lv, Fu, Shi, Yang, & Han, 2017). Hence, this technique is suitable to screen for potential ACE2 ligands.

In this study, we used human embryonic kidney 293T cells highly expressing stable ACE2 receptors (ACE2-HEK293T cells) to screen *Scutellaria* plants for potential ACE2 blockers that could bind to ACE2. Then, relevant biological methods were used to confirm the affinity and anti-COVID-19 effects of the screened compounds.

2 | MATERIALS AND METHODS

2.1 | Materials and reagents

ACE2-HEK293T cells were purchased from Genomeditech (item No. GM-CS-108841, Shanghai, China). Dulbecco's modified Eagle's medium (DMEM) with high glucose (Cat. No. SH30022.01), and fetal bovine serum (FBS; Cat. No. 16140071) were purchased from HyClone (Logan, UT). Penicillin–streptomycin solution was obtained from Xi'an Hat Biotechnology Co., Ltd. (Xi'an, China). ACE2 cells were maintained in DMEM with high glucose containing 10% FBS, 1% penicillin–streptomycin, and 4 μg/ml puromycin and cultured at 37°C in a 5% CO_2 incubator.

Annexin V-fluorescein isothiocyanate (FITC)/propidium iodide (PI) apoptosis detection kit (Cat. No. A005-3) and the cell counting kit-8 (CCK-8) were purchased from 7Sea Pharmatech Co., Ltd. (Shanghai, China). The SARS-CoV-2-spiked pseudotyped virus (Cat: PSV001) was purchased from Sino Biological (Beijing, China). Protease and phosphatase inhibitor cocktails were purchased from Roche Diagnostics (Mannheim, Germany). The 5× loading buffer was purchased from Thermo Fisher Scientific, Inc. (MA), and sodium dodecyl sulfate-polyacrylamide gel electrophoresis (SDS-PAGE) apparatus was obtained from Pioneer Biotech Co., Ltd. (Xi'an, China).

Polyvinylidene fluoride (PVDF) membranes were obtained from Hangzhou Microna Membrane Technology Co., Ltd. (Hangzhou, China). The following antibodies and reagents were used: anti-light chain 3 (LC3) rabbit polyclonal antibody (14600-1-AP, Proteintech Group Inc., Rosemont, IL), anti-glyceraldehyde 3-phosphate dehydrogenase (GAPDH, 1:2,000, #2118, CST), tetramethylrhodamine isothiocyanate (TRITC) phalloidin (40734ES75, 40734ES80, Yeasen), CoraLite488-conjugated Affinipure goat anti-rabbit immunoglobulin G (IgG, H + L; SA00013-2, Proteintech Group Inc.), 4′,6-diamidino-2-phenylindole (DAPI)-Fluoromount-G™ (0100–20, Pioneer Biotechnology), 5× loading sample buffer (Thermo Fisher Scientific, Inc.), and enhanced chemiluminescence (ECL) kit (Proteintech Group, Inc.).

The calcium imaging buffer (CIB) contained 125 mM sodium chloride (NaCl), 3 mM potassium chloride (KCl), 2.5 mM calcium chloride ($CaCl_2$), 0.6 mM magnesium chloride ($MgCl_2$), 10 mM HEPES, 20 mM glucose, 1.2 mM sodium bicarbonate ($NaHCO_3$), and 20 mM sucrose, and the pH was buffered close to 7.4. Fluo-3, AM ester, and Pluronic F-127 acid were obtained from Biotium (CA). Oroxylin A, wogonin, scutellarin, and neobaicalein (purity 98%) were purchased from Chengdu Pufeide Biotech Co., Ltd. (Chengdu, Sichuan, China).

2.2 | Preparation of ACE2/CMC stationary phase

Approximately 1×10^7 ACE2 cells were collected, washed with physiological saline (pH 7.4), and centrifuged at 3,000×*g* for 10 min at 4°C; this process was performed twice. Then, the cells were disrupted using a sonicator for 30 min on ice, homogenized using an ultrasonic disintegrator according to the set procedure for 3 min, and centrifuged at 1,000×*g* for 10 min at 4°C. Then, the precipitate was discarded, the supernatant was centrifuged at 12,000×*g* for 20 min at 4°C, and 10 ml saline was added to resuspend the pellet, followed by centrifugation at 12,000×*g*.

The ACE2 cell membrane pellet was resuspended with 5 ml saline, which was slowly added to a test tube containing silica gel (50 mg, activated at 105°C for 30 min) under reduced pressure and vibration, and allowed to react for 5 min. The reaction mixture was transferred to a 10-ml centrifuge tube on ice. A magnetic stirrer was used to stir the mixture of the cell-membrane preparation and silica gel at 4°C for 30 min, after which it was allowed to stand overnight to

produce a uniformly wrapped ACE2 cell membrane stationary phase. Lastly, the cell membrane stationary phase was loaded into the CMC column (10 mm × 2.0 mm i.d.).

2.3 | ACE2/CMC column preparation

The cell membrane stationary phase suspension was vortexed, centrifuged at 500×*g* for 10 min at 4°C. The supernatant was discarded and 5 ml of saline was added to the pellet, followed by vortexing. This process was repeated to remove the excess cell membranes that were not wrapped around the silica gel. Approximately 5 ml of physiological saline was added to the precipitate, followed by vortexing, and then the mixture was poured into a pre-washed column packer. The flow rate of the mobile phase (water) was set to 2.0 ml/min. When the pressure of the column was not more than 10 MPa and the column was loaded for 5 min, the cell membrane stationary phase was loaded into the column core and the packed CMC column was used for liquid chromatography.

2.4 | Chromatographic conditions

Chromatography was performed using an Acchrom instrument (Model 56000, Huapuke Instrument, Beijing Technology Co., Ltd.). Deionized water was used as the mobile phase at a flow rate of 0.2 ml/min. The column temperature was set at 37°C, and 5 μl of the sample was used as the injection volume. A diode array detector was used for full wavelength detection.

2.5 | Frontier analysis

For chromatography, the column was first equilibrated with deionized water for 1 hr. Solution B was prepared by dissolving melaleuca glycoside A in solution A at a concentration of 1×10^{-6} M, which was then further diluted to solutions of 2.5×10^{-8} M, 5×10^{-8} M, 1×10^{-7} M, 2×10^{-7} M, 4×10^{-7} M, 6×10^{-7} M, and 8×10^{-7} M. Solutions of varying concentrations were injected into the chromatographic column from low to high and when equilibrium was reached, the curve achieved a plateau phase, thereby creating a breakthrough curve. Then, the mobile phase was then switched to 100% solution A for elution, followed by the next concentration for the adsorption and elution process. This process was continued until eight different breakthrough curves were obtained. In the CMC model, the K_D was calculated by the regression curves according to Ma's method (Ma et al., 2017).

2.6 | Cytotoxicity

ACE2 and HEK293T cells were cultured in DMEM high-glucose medium containing 10% serum and 1% antibiotics in an incubator at 37°C in an atmosphere of 5% CO_2. The CCK-8 assay was used to detect the effects of oroxylin A, wogonin, scutellarin, and neobaicalein on cell viability at various concentrations and treatment durations. The cell suspension was inoculated into a 96-well plate in a 37°C incubator overnight and then treated with oroxylin A, wogonin, scutellarin, and neobaicalein at concentrations of 0.1, 1, 10, 50, 100, 200, 300, 400, 500, 600, and 800 μM in DMEM, followed by incubation at 37°C in an incubator for 24 hr.

Cells cultured in the medium and the medium without any cells were used as the negative control and blank control groups, respectively. After treatment with the compounds, CCK-8 solution was added, followed by incubation at 37°C for 2 hr, and then the optical density (OD) of the samples was measured at a wavelength of 450 nm.

2.7 | Detection of SARS-CoV-2-spiked pseudotyped virus entry into ACE2 cells

ACE2 cells (5×10^4/well) were seeded into white 96-well plates in 100 μl DMEM per well and cultured at 37°C in an incubator with 5% CO_2 for 24 hr. The cells were treated with 100 μl of medium containing the corresponding concentration of the test substances for 2 hr and 5 μl of the SARS-CoV-2-spiked pseudotyped virus (Cat PSV001, Sino Biological), followed by incubation for further infection for 10 hr at 37°C in an incubator with 5% CO_2. Then, the culture medium containing the virus was removed and replaced with 200 μl of fresh DMEM, followed by continuous incubation at 37°C for 48 hr. The culture medium was subsequently aspirated from the 96-well plate. Then, 20 μl of the cell lysate solution from the Luciferase assay system 100 assays (Promega, E1500) was added to each well, followed by 100 μl of the luminescence solution before the detection of luciferase luminescence. The exposure time was 1 s.

2.8 | Apoptosis

ACE2 cells were seeded in a six-well plate and treated with different concentrations of oroxylin A (0, 20, 40, and 80 μM). A blank control, Annexin V-FITC single staining, and PI single staining groups were also established. The cells were cultured for 24 hr, after which the culture medium was washed out with phosphate-buffered saline (PBS) and the cells were washed once with PBS. Next, the cells were digested with trypsin and the culture medium was collected, blown gently, transferred to a centrifuge tube, and centrifuged at 500×*g* for 5 min.

After discarding the supernatant, the cells were resuspended in 1 ml of PBS, counted to ensure the number was not less than 10^5, centrifuged at 500×*g* for 5 min, and then collected. Next, 400 μl of a 1× binding buffer was added to resuspend the cells, the suspension was centrifuged at 500×*g* for 5 min. Five microliters of Annexin V-FITC was added to the suspension, mixed well, and incubated for 15 min at room temperature in the dark. Then, 10 μl of PI dye solution was added, mixed well, and the mixture was incubated for 5 min in an ice bath in the dark.

The suspension was examined using flow cytometry within 30 min at excitation and emission wavelengths of 488 and 530 nm, respectively to detect FITC and >575 nm to detect PI. Normal cells showed only very low fluorescence intensity whereas apoptotic cells exhibited strong green fluorescence. Necrotic cells were double-stained with green and red fluorescence.

2.9 | Immunofluorescence assay

Cell samples were prepared using 24 mm × 24 mm coverslips, which were sterilized with 75% ethanol and coated with polylysine. Then, 2×10^3 ACE2 cells were seeded on the coverslips and cultured in a six-well plate, which was incubated overnight at 37°C in an incubator flushed with 5% CO_2. Then, the cells were treated with 10, 20, or 40 μM of oroxylin A dissolved in serum-free DMEM for 24 hr. The cells were fixed with 4% paraformaldehyde for 10 min at room temperature, washed with PBS, incubated with 0.5% Triton X-100 for 5 min followed by incubation with 5% BSA for 1 hr at room temperature, and washed three times with PBS. Next, the cells were incubated with the LC3 primary antibody at 37°C for 3 hr, followed by treatment with the fluorescent secondary antibody at room temperature for 2 hr. Then, the cells were treated with TRITC-phalloidin for 30 min at room temperature and mounted with 50 μl of DAPI-containing anti-fluorescence quenching reagent. Cells were visualized using laser confocal fluorescence microscopy.

2.10 | Western blot assay

ACE2 cells were treated with 10, 20, or 40 μM oroxylin A in serum-free DMEM for 24 h, and the total protein were extracted by adding RIPA lysis buffer containing 10% protease inhibitor and a phosphatase inhibitor cocktail (Roche Diagnostics) on ice for 30 min. The insoluble protein lysate was removed by centrifuging the samples at 13,500×*g* for 10 min at 4°C and the protein concentration was determined using a bicinchoninic acid protein quantification kit according to the manufacturer's instructions.

The protein in the cell lysates was denatured by boiling the samples with 5× loading sample buffer (Thermo Fisher Scientific, Inc., MA) for 5 min, and equal amounts of protein were separated using 15% sodium dodecyl sulfate-polyacrylamide gel electrophoresis (SDS-PAGE; Shaanxi Pioneer Biotech Co., Ltd.). The separated proteins were transferred onto PVDF membranes (Hangzhou Microna Membrane Technology Co., Ltd., Hangzhou, China), which were blocked using 5% non-fat milk in Tris-buffered saline containing Tween-20 (TBST; Shaanxi Pioneer Biotech Co., Ltd.) for 2 hr at room temperature with continuous agitation.

The membranes were then incubated overnight at 4°C with anti-LC3 (1:1,000) and anti-GAPDH (1:2,000) primary antibodies. The membranes were then washed three times with TBST for 10 min each time, incubated with secondary antibodies (1:20,000) in TBST for 1 hr at 37°C, washed three times with TBST for 10 min each, and developed using an ECL kit. Image-Pro Plus 5.1 software (Media Cybernetics, Inc., Rockville, MD) was used to quantify the protein levels.

2.11 | Intracellular Ca^{2+} mobilization assay

All compounds were diluted to the required concentration using CIB. The incubation buffer contained 4 μM Fluo-3 AM and 0.1% Pluronic F-127. For imaging, cells were washed twice with CIB and imaged at excitation wavelengths of 488 nm. Unless otherwise specified, compounds were added to the well at 10 s after initial imaging, and responses were monitored for an additional 120 s over 1-s intervals. The cells were identified as responding if $[Ca^{2+}]$ increased by at least 50% after the substances were injected.

2.12 | Surface plasmon resonance assay

ACE2 protein with 6× His tag (30 μg/ml) was fixed on the —COOH sensor chip using capture-coupling and then, 10, 20, 40, and 80 μM oroxylin A was injected sequentially into the chamber with PBS running buffer. The interaction of ACE2 with the fixed small molecules was detected using Open SPR™ (Nicoya Lifesciences, Waterloo, Canada) at 25°C. The binding and dissociation times were both 250 s, the flow rate was 20 μl/s, and the chip was regenerated with hydrochloric acid (pH 2.0). A one-to-one diffusion corrected model was fit to the wavelength shifts corresponding to the various compound concentrations and the data were analyzed using TraceDrawer software (Yang et al., 2018).

2.13 | Molecular docking

To investigate the interactions between the receptor and ligand, molecular docking studies were conducted using the Sulflex-Dock Mode of Sybyl-X program package (New Tripos International, St. Louis, MO). The docking model of ACE2 used in this study was based on the homology model of ACE2 reported by Dr. Michael W. Pantoliano (Towler et al., 2004). The predicted ACE2 structure was used to dock oroxylin A and the reported ACE2 ligand MLN-4760.

2.14 | Statistical analysis

The data are presented as the means ± SD and were statistically analyzed using a one-way analysis of variance. The differences were considered statistically significant at $p < .05$.

2.15 | Statement

For this experiment, many requirements considered to be relevant have been taken into account in recent guidelines for best practice in natural products pharmacological research (Heinrich et al., 2020; Izzo et al., 2020).

3 | RESULTS

3.1 | Screening of bioactive components of Radix Scutellariae using ACE2/CMC

CMC is a biological affinity chromatography used to demonstrate receptor–ligand binding. In this study, the ACE2/CMC method was used to screen oroxylin A isolated from *Radix Scutellariae* extract (Figure 1A). The retention times of oroxylin A, wogonin, scutellarin, and neobaicalein were determined to be 10.90, 5.46, 4.37, and 2.97 min, respectively (Figure 1B), which indicated that oroxylin A was the best ACE2 ligand among the four compounds. Next, ACE2/CMC combined with the frontier analysis method was used to calculate the K_D of the binding of oroxylin A to ACE2. Regression curves were drawn based on the breakthrough curves of oroxylin A and the K_D value was subsequently calculated as the ratio of the intercept to the slope (Figure 1C,D).

3.2 | Cytotoxicity of components on ACE2 cells

A CCK-8 assay was used to detect the effects of oroxylin A, wogonin, scutellarin, and neobaicalein on ACE2 cell viability. The half-maximal inhibitory concentration (IC_{50}) values of oroxylin A, wogonin, scutellarin, and neobaicalein were determined to be 164.6, 137.6, 170.9, and 1 83.8 μM, respectively (Table 1). Treatment with 0, 20, 40, and 80 μM of oroxylin A showed almost no apoptotic effect on ACE2 cells (Figure 2).

3.3 | Oroxylin A suppressed entrance of SARS-CoV-spiked pseudotyped virus into ACE2 cells

ACE2 cells were treated with 20 μM oroxylin, wogonin, scutellarin, and neobaicalein to detect their anti-invasive effects on SARS-CoV-2-spiked pseudotype virus. For this experiment, the luciferase luminescence value was defined as 1 for the control group treated with the same solvent without any antagonistic compounds, and the anti-invasive effect was expressed as a ratio to that of the control group. Chloroquine (CQ) was used as a positive control. The results showed that the SARS-CoV-2-spiked pseudotype virus penetration ratio was 0.2426 ± 0.0342, 0.8704 ± 0.0857, 0.9023 ± 0.1619, 2.685 ± 0.0634, and 0.3266 ± 0.0495 for oroxylin A, wogonin, scutellarin, neobaicalein, and CQ, respectively (Figure 3A). Treatment with 10 and 40 μM oroxylin A and 20 μM CQ reduced the SARS-CoV-2-spiked pseudotype virus penetration ratio to 0.6173 ± 0.0494,

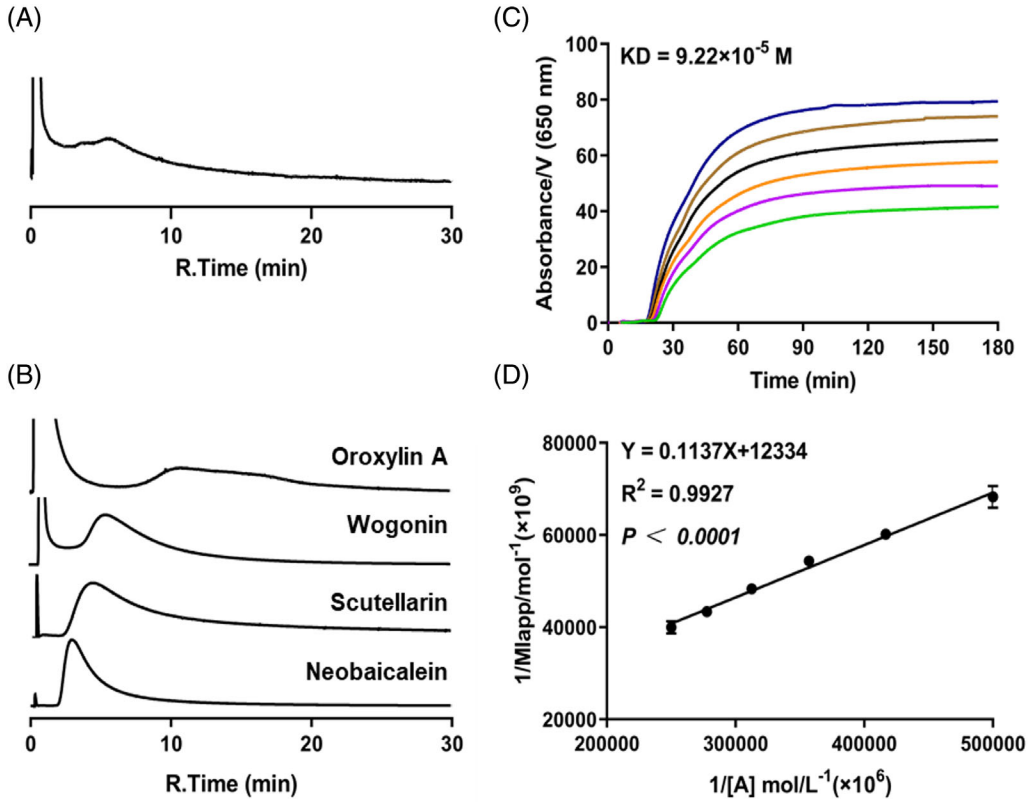

FIGURE 1 Bioactive components of Radix Scutellariae screened using angiotensin-converting enzyme II (ACE2)/cell membrane chromatography (CMC). ACE2/CMC of (A) Radix Scutellariae extract and (B) reported active ingredients of oroxylin A, wogonin, scutellarin, and neobaicalein. (C) ACE2/CMC breakthrough curves of oroxylin A. (D) Regression curves constructed using plotting m_{Lapp} versus 1/[*A*], and concentrations of oroxylin A were 2×10^{-6} M, 2.4×10^{-6} M, 2.8×10^{-6} M, 3.2×10^{-6} M, 3.6×10^{-6} M, and 4×10^{-6} M (from bottom to top), respectively. Experiments were performed three times [Colour figure can be viewed at wileyonlinelibrary.com]

0.2426 ± 0.0342, and 0.5052 ± 0.0258, respectively (Figure 3B). The ability of the SARS-CoV-2-spiked pseudotype virus to enter ACE2 cells was reduced significantly, indicating that oroxylin A could effectively prevent COVID-19 via its interaction with ACE2.

3.4 | Oroxylin A inhibits LC3-mediated autophagy of ACE2 cells

The autophagosome is a spherical structure. LC3, which is an important marker of autophagosomes, is known to be related to its stability. After treatment with 10, 20, and 40 μM of oroxylin A, ACE2 cells were stained with FITC-LC3, TRITC-phalloidin, and DAPI (Figure 4A).

TABLE 1 The IC_{50} of the components on ACE2 cells

Components	Oroxylin	Wogonin	Scutellarin	Neobaicalein
IC_{50} (μM)	164.6	137.6	170.9	83.8

The results indicated that oroxylin A inhibited LC3 expression. LC3 consists of LC3-I and LC3-II, which are located in the cytoplasm and membrane, respectively. LC3-II is converted from LC3-I to initiate the formation and elongation of autophagosomes. Oroxylin A down-regulated LC3-II expression and the ratio of LC3-II to LC3-I, indicating the inhibitory effect of LC3-II-mediated autophagy (Figure 4B,C).

3.5 | Oroxylin A did not trigger Ca^{2+} influx in ACE2-expressing cells

To confirm the effects of oroxylin A on the Ca^{2+} influx, ACE2-HEK293 cells were treated with 20, 40, and 80 μM of oroxylin A. HEK293T cells treated with 80 μM of oroxylin A was used as the control group. Ca^{2+} influx was detected using a Ca^{2+} mobilization assay with Fluo-3, AM as the Ca^{2+} labeling reagent. The results suggested that Ca^{2+} influx was not triggered in ACE2-expressing (Figure 5A–C) and HEK293T cells (Figure 5D).

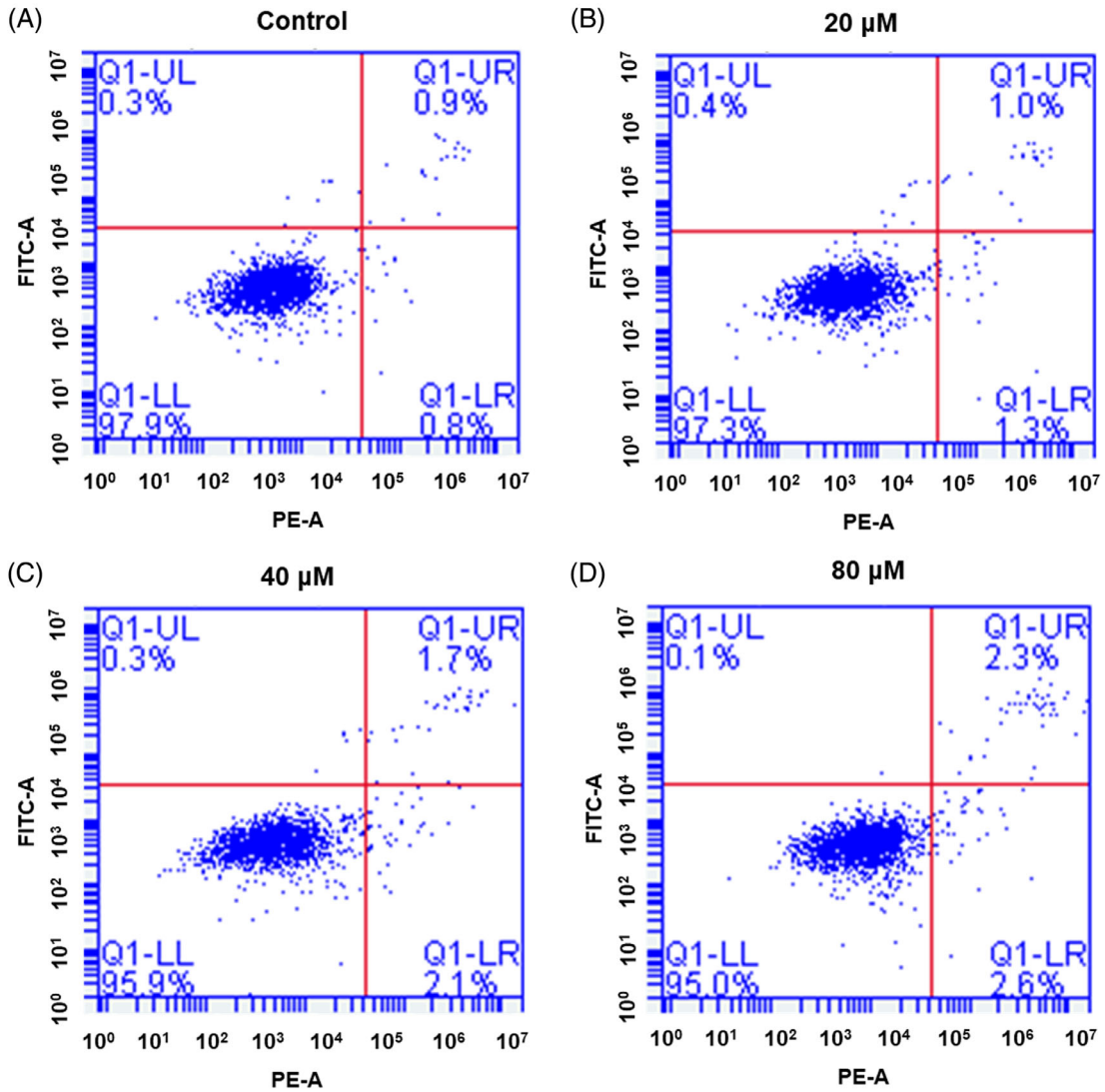

FIGURE 2 Effect of oroxylin A on HEK293T cells stably expressing angiotensin-converting enzyme II (ACE2 cells). ACE2 cells were treated with 0, 20, 40, and 80 μM oroxylin A for 24 hr, and cell apoptosis was detected using Annexin V-fluorescein isothiocyanate (FITC)/propidium iodide (PI) apoptosis detection kit. Each experiment was performed three times [Colour figure can be viewed at wileyonlinelibrary.com]

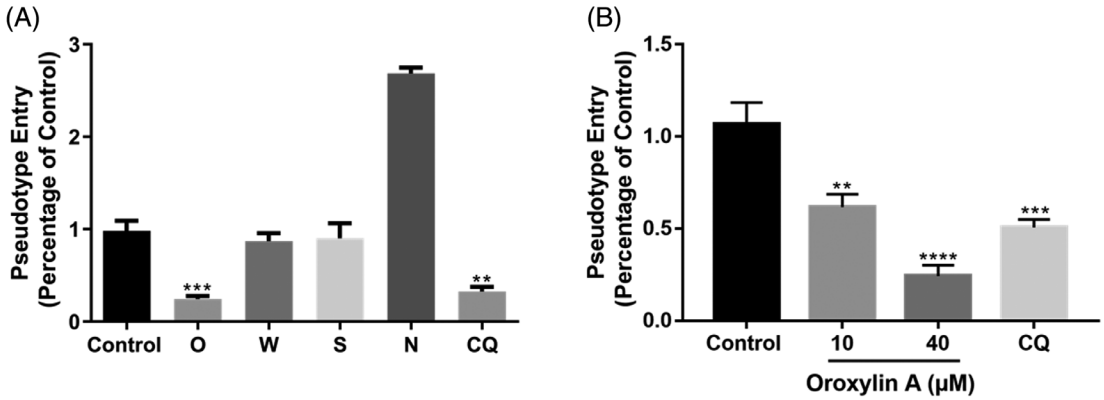

FIGURE 3 Effects of compounds on the entrance of severe acute respiratory syndrome coronavirus-2 (SARS-CoV-2)-spiked pseudotyped virus into HEK293T cells stably expressing angiotensin-converting enzyme II (ACE2 cells). (A) Effect of 20 μM oroxylin A (O), wogonin (W), scutellarin (s), and neobaicalein (N). (B) Dose-dependent effect of oroxylin A on ACE2 cells treated with 10 and 20 μM oroxylin A. Each experiment was repeated three times. Data are expressed as means ± SD, $^{**}p < .01$ and $^{***}p < .001$ versus control

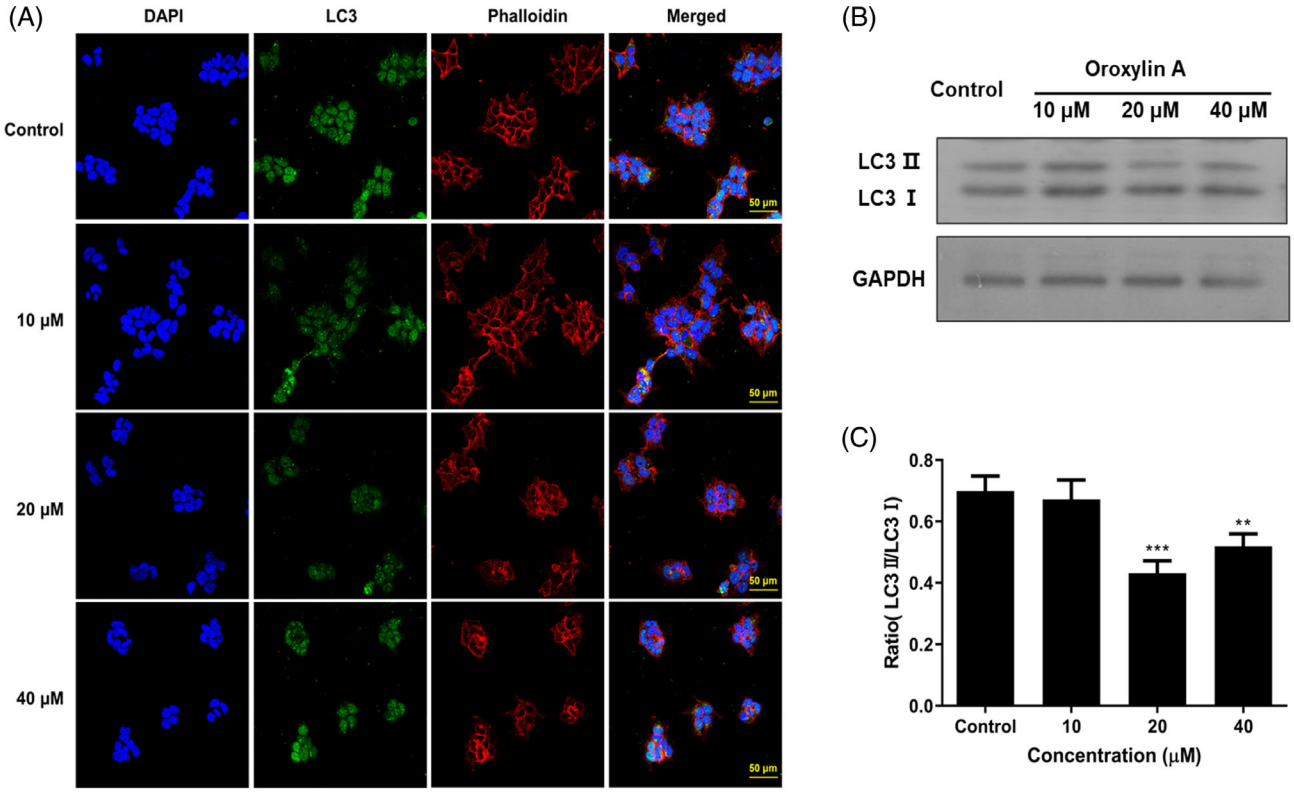

FIGURE 4 Effects of oroxylin A on light chain 3 (LC3) levels of HEK293T cells stably expressing angiotensin-converting enzyme II (ACE2 cells). ACE2 cells were treated with 0, 10, 20, and 40 μM oroxylin A for 24 hr. (A) Effects of oroxylin A on immunofluorescence staining of fluorescein isothiocyanate (FITC)-LC3 and tetramethylrhodamine isothiocyanate (TRITC)-phalloidin in ACE2 cells. Scale bar, 50 μm. (B) Representative blots of LC3-II and LC3-I-related autophagy changes. (C) Quantification of LC3-II/LC3-I ratio in (B). Each experiment was performed three times. Data are expressed are means ± SD; $^{**}p < .01$ and $^{***}p < .001$ versus control [Colour figure can be viewed at wileyonlinelibrary.com]

3.6 | Binding ability of oroxylin A to the ACE2 receptor

Based on the molecular docking results, MLN-4760 formed a hydrogen bond with ARG518 (2.66 Å long), HIS374 (2.22 Å long), SER409 (2.00 Å long), and GLU406 (2.11 Å and 1.94 Å long) of ACE2 (Figure 6A). Oroxylin A formed a hydrogen bond with the ASN290 (1.95 Å long) and ASP367 (2.19 Å and 2.06 Å long) of ACE2 (Figure 6B). The ribbon model of oroxylin A and ACE2 shows that the affinity of oroxylin A (4.7562) for hydrogen bonds might be correlated

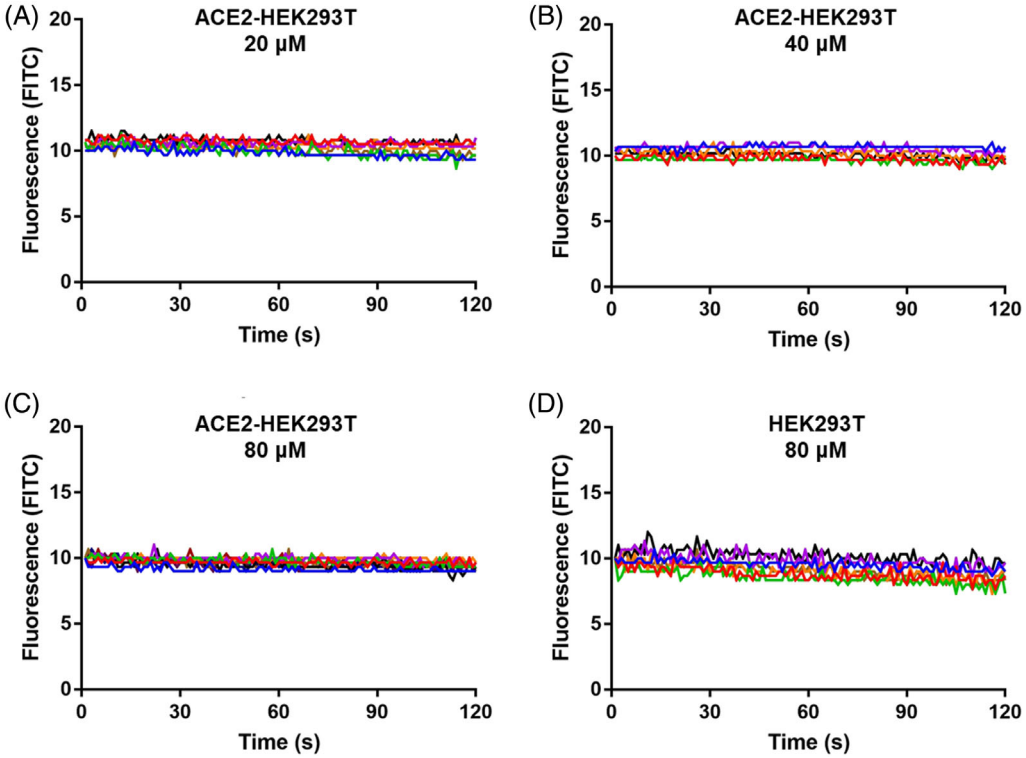

FIGURE 5 Effects of oroxylin A on Ca^{2+} influx. (A–C) HEK293T cells stably expressing angiotensin-converting enzyme II (ACE2 cells) were treated with 20, 40, and 80 μM oroxylin A, and Ca^{2+} influx was detected using intracellular Ca^{2+} mobilization assay. (D) Ca^{2+}-influx effect of HEK293T cells treated with 80 μM oroxylin A. Each experiment was performed three times [Colour figure can be viewed at wileyonlinelibrary.com]

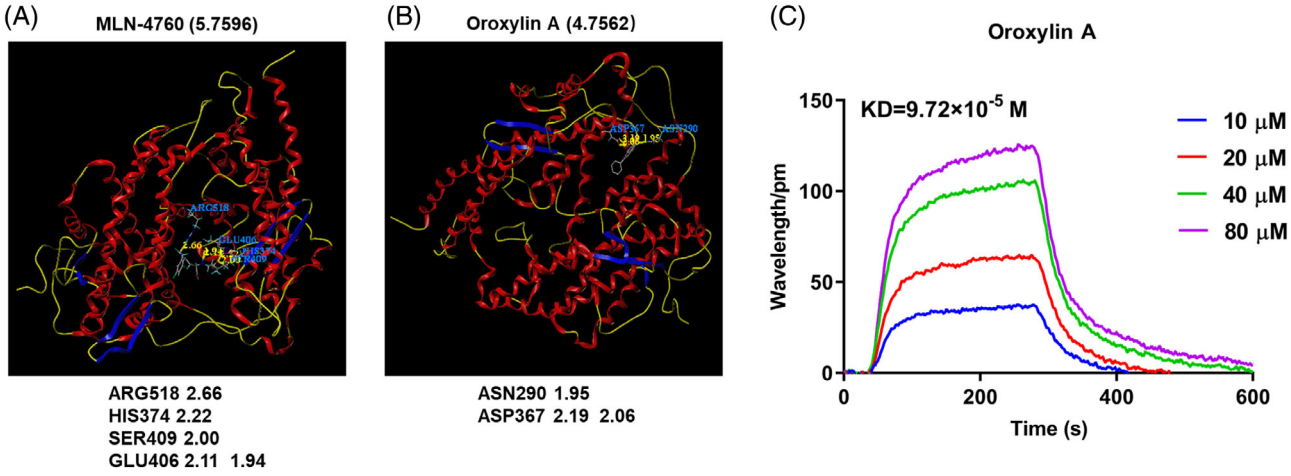

FIGURE 6 Interaction between oroxylin A and angiotensin-converting enzyme II (ACE2). Schematic diagram of binding between oroxylin A and ACE2 determined using molecular docking. Ribbon models of (A) represent ACE2 ligand MLN-4760 binding to ACE2 and (B) oroxylin A binding to ACE2. (C) Binding curves of oroxylin A on ACE2-COOH sensor chip using surface plasmon resonance (SPR). Each experiment was performed three times [Colour figure can be viewed at wileyonlinelibrary.com]

with its affinity for MLN-4760 (5.7596), indicating that oroxylin A showed an appreciable binding ability to ACE2. Surface plasmon resonance (SPR) analysis confirmed that oroxylin A could bind to ACE2; the K_D of oroxylin A was calculated to be 9.72×10^{-6} M using TraceDrawer™ (Figure 6D).

4 | DISCUSSION

COVID-19 is a prevalent global pandemic and, currently, there is no specific drug to cure the infection or as a prophylactic. The TCM preparation, Radix Scutellariae, has shown curative effects against some

diseases in a clinical setting. In this study, we examined the pharmacodynamic effects of the SARS-CoV-2-spiked pseudotyped virus blocker, oroxylin A. This compound was obtained after screening Radix Scutellariae using the ACE2/CMC method and was found to have promising effects.

The manifestation of COVID-19 ranges from a mild, self-limiting respiratory tract illness to severe progressive pneumonia, multiorgan failure, and death (Huang et al., 2020). The spike (S) proteins of coronaviruses, including the coronavirus that causes SARS such as COVID-19, are associated with cellular receptors that mediate the infection of their target cells. ACE2, a carboxypeptidase that potently degrades angiotensin II to angiotensin 1–7, has been identified as a functional receptor for SARS-CoV (Li et al., 2003) and a potent receptor for the entrance of this virus into cells (Yan et al., 2020; Zhou et al., 2020).

ACE2 is currently recognized as a target of SARS-CoV-2 (Skarstein Kolberg, 2020). In this study, an ACE2 high-expression CMC system was established to screen the potential ACE2 ligands and investigate their binding properties. Oroxylin A obtained from Radix Scutellariae had a longer retention time in the ACE2-CMC system than that of neobaicalein, scutellarin, and wogonin. Oroxylin A has been reported to have potential antiviral effects (Jin et al., 2018); however, its mechanism against SARS-CoV-2 has not yet been elucidated.

First, we investigated the cytotoxicity of oroxylin A, neobaicalein, scutellarin, and wogonin and found that they all showed less toxicity at lower concentrations. Therefore, follow-up in vitro studies were conducted using a low concentration range of the test compounds. SARS-CoV-spiked pseudotyped viruses are useful virological tools because of their safety and versatility, especially for emerging and re-emerging viruses (Nie et al., 2020). The SARS-CoV-2-spiked pseudotyped virus experiment showed that oroxylin A had strong anti-pseudotyped virus activity, which showed a dose-dependent effect in subsequent experiments, whereas neobaicalein, scutellarin, and wogonin did not exhibit this effect.

To further investigate the autophagic and apoptotic effects of oroxylin A, we measured filamentous actin and LC3 expression using immunofluorescence and the expression of autophagy-related proteins LC3-I and LC3-II using western blotting. Autophagy plays a crucial role in immune responses, cellular metabolism, apoptosis, and cell death (Choi, Ryter, & Levine, 2013). The expression of LC3 protein expression is an important indicator of autophagy (Klionsky et al., 2016). The conversion of LC3-I to LC3-II plays an important role in the activation of autophagy (Chen et al., 2010).

Our results demonstrated that oroxylin A decreased LC3-mediated autophagy, which suggested that oroxylin A effectively decreased autophagy in ACE2 cells. We found that oroxylin A, at concentrations below 80 μM, had no effect on inducing apoptosis in ACE2-expressing cells. Studies have identified a close relationship between autophagy and the inflammatory response (Zhong, Sanchez-Lopez, & Karin, 2016). Ca^{2+} influx analysis using the intracellular Ca^{2+} mobilization assay showed that oroxylin A had no Ca^{2+}-influx effect on ACE2 expression and HEK293T cells.

Of late, molecular docking has been widely used for the identification of antiviral compounds effective against SARS-CoV-2. For example, the structure of SARS-CoV-2 $3CL^{pro}$ (3-chymotrypsin-like cysteine protease), which controls coronavirus replication and is essential for its life cycle, has been used to identify anti-COVID-19 components from medicinal plants (Tahir Ul Qamar, Alqahtani, Alamri, & Chen, 2020). The essential residues and ligand-receptor interactions of the peptide-like structure of the main protease inhibitors of SARS-CoV-2 have been identified using the co-crystallized structures of SARS-CoV-2 with the main protease (6Y2F and 6W63) (Pant, Singh, Ravichandiran, Murty, & Srivastava, 2020). The modeled RNA-dependent RNA polymerase (RdRp) of COVID-19 has been targeted using different anti-polymerase ingredients available commercially, which have been approved for use as antivirals (Elfiky, 2020). In this study, molecular docking studies were used to investigate ligand-protein interactions between ACE2 and oroxylin A. The ribbon model of oroxylin A and ACE2 indicated that the affinity of oroxylin A to ACE2 might be correlated with hydrogen bonds, indicating that they showed good binding ability. SPR analysis further confirmed that oroxylin A binds to the ACE2 protein with a K_D of 9.72×10^{-6} M, which was calculated using TraceDrawer™. These results proved that the binding effect of ACE2 determined using CMC was consistent with the anti-SARS-CoV-2-spiked pseudotyped virus effect identified in ACE2-expressing cells. CMC and the SPR assay demonstrated the binding properties of oroxylin A to ACE2 from different perspectives, and both enabled a consistent conclusion to be drawn.

5 | CONCLUSIONS

Our findings indicated the anti-SARS-CoV-2-Spike pseudotyped virus infection activity of Oroxylin A on ACE2 cells. Hence, Oroxylin A is a promising new candidate for the treatment of COVID-19.

ACKNOWLEDGMENTS

The authors thank Miss. Jue Wang, Jia Fu, and Qianqian Jia for their contributions to a screening of potential candidate against 2019-nCoV and support for the current research, as well as Xiaowei Li for the help and support of this study. This work was supported by the National Natural Science Foundation of China (Grant numbers: 81930096 and 81903572) and China Postdoctoral Science Foundation (Grant number: 2019M663755).

AUTHOR CONTRIBUTIONS

Rui Liu and Yuanyuan Ding participated in research design. Jiapan Gao, Yuanyuan Ding, Yuejin Wang, Liyang Zhang and Peida Liang conducted experiments. Jiapan Gao, Yuanyuan Ding, Yuejin Wang, Peida Liang and Rui Liu performed data analysis. Rui Liu and Yuanyuan Ding wrote or contributed to the writing of the manuscript.

CONFLICT OF INTEREST

The authors declare no competing financial interests.

ORCID

Rui Liu https://orcid.org/0000-0003-1235-4263

REFERENCES

Chen, S., Rehman, S. K., Zhang, W., Wen, A., Yao, L., & Zhang, J. (2010). Autophagy is a therapeutic target in anticancer drug resistance. *Biochimica et Biophysica Acta*, *1806*(2), 220–229.

Choi, A. M., Ryter, S. W., & Levine, B. (2013). Autophagy in human health and disease. *New England Journal of Medicine*, *368*(7), 651–662.

Elfiky, A. A. (2020). Ribavirin, Remdesivir, Sofosbuvir, Galidesivir, and Tenofovir against SARSCoV-2 RNA dependent RNA polymerase (RdRp): A molecular docking study. *Life Science*, *258*, 118350.

Han, S., Lv, Y., Wei, F., Fu, J., Hu, Q., & Wang, S. (2018). Screening of bioactive components from traditional Chinese medicines using cell membrane chromatography coupled with mass spectrometry. *Phytochemical Analysis*, *29*(4), 341–350.

Heinrich, M., Appendino, G., Efferth, T., Fürst, R., Izzo, A. A., Kayser, O., … Viljoen, A. (2020). Best practice in research – Overcoming common challenges in phytopharmacological research. *Journal of Ethnopharmacology*, *246*, 112230.

Ho, J. C., Ooi, G. C., Mok, T. Y., Chan, J. W., Hung, I., Lam, B., … Tsang, K. W. (2003). High-dose pulse versus nonpulse corticosteroid regimens in severe acute respiratory syndrome. *American Journal of Respiratory and Critical Care Medicine*, *168*, 1449–1456.

Holshue, M. L., DeBolt, C., Lindquist, S., Lofy, K. H., Wiesman, J., Bruce, H., … Pillai, S. K. (2020). First case of 2019 novel coronavirus in the United States. *New England Journal of Medicine*, *382*, 929–936.

Huang, C., Wang, Y., Xingwang, L., Lili, R., Zhao, J., Hu, Y., … Cao, B. (2020). Clinical features of patients infected with 2019 novel coronavirus in Wuhan, China. *The Lancet*, *395*(10223), 497–506.

Izzo, A. A., Teixeira, M., Alexander, S. P. H., Cirino, G., Docherty, J. R., George, C. H., … Ahluwalia, A. (2020). A practical guide for transparent reporting of research on natural products in the British Journal of pharmacology: Reproducibility of natural product research. *British Journal of Pharmacology*, *177*(10), 2169–2178.

Jia, Q. Q., Sun, W., Zhang, L. Y., Fu, J., Lv, Y., Lin, Y., & Han, S. (2019). Screening the anti-allergic components in Saposhnikoviae Radix using high-expression Mas-related G protein-coupled receptor X2 cell membrane chromatography online coupled with liquid chromatography and mass spectrometry. *Journal of Separation Science*, *42*(14), 2351–2359.

Jin, J., Chen, S., Wang, D., Chen, Y., Wang, Y., Guo, M., … Dou, J. (2018). Oroxylin A suppresses influenza A virus replication correlating with neuraminidase inhibition and induction of IFNs. *Biomedicine & Pharmacotherapy*, *97*, 385–394.

Jin, Y. H., Cai, L., Cheng, Z. S., Cheng, H., Deng, T., Fan, Y. P., … Wang, X. H. (2020). A rapid advice guideline for the diagnosis and treatment of 2019 novel coronavirus (2019-nCoV) infected pneumonia (standard version). *Military Medical Research*, *7*, 4.

Kitamura, K., Honda, M., Yoshizaki, H., Yamamoto, S., Nakane, H., Fukushima, M., … Tokunaga, T. (1998). Baicalin, an inhibitor of HIV-1 production in vitro. *Antiviral Research*, *37*(2), 131–140.

Klionsky, D. J., Abdelmohsen, K., Abe, A., Abedin, M. J., Abeliovich, H., Acevedo Arozena, A., … Zughaier, S. M. (2016). Guidelines for the use and interpretation of assays for monitoring autophagy (3rd edition). *Autophagy*, *12*(1), 1–222.

Lee, N., Hui, D., Wu, A., Chan, P., Cameron, P., Joynt, G. M., … Sung, J. J. (2003). A major outbreak of severe acute respiratory syndrome in Hong Kong. *New England Journal of Medicine*, *348*, 1986–1994.

Li, H. B., Jiang, Y., & Chen, F. (2004). Separation methods used for *Scutellaria baicalensis* active components. *Journal of Chromatography. B, Analytical Technologies in the Biomedical and Life Sciences*, *812*(1–2), 277–290.

Li, W., Michael, J. M., Natalya, V., Sui, J., Wong, S. K., Berne, M. A., … Farzan, M. (2003). Angiotensin-converting enzyme 2 is a functional receptor for the SARS coronavirus. *Nature*, *426*(6965), 450–454.

Liang, S., Deng, X., Lei, L., Zheng, Y., Ai, J., Chen, L., … Ren, Y. (2019). The comparative study of the therapeutic effects and mechanism of Baicalin, Baicalein, and their combination on ulcerative colitis rat. *Frontiers in Pharmacology*, *10*, 1466.

Lin, Y., Lv, Y., Fu, J., Jia, Q., & Han, S. (2018). A high expression mas-related G protein coupled receptor X2 cell membrane chromatography coupled with liquid chromatography and mass spectrometry method for screening potential anaphylactoid components in kudiezi injection. *Journal of Pharmaceutical and Biomedical Analysis*, *159*, 483–489.

Lv, Y., Fu, J., Shi, X., Yang, Z., & Han, S. (2017). Screening allergic components of Yejuhua injection using LAD2 cell membrane chromatography model online with high performance liquid chromatography-ion trap-time of flight-mass spectrum system. *Journal of Chromatography. B, Analytical Technologies in the Biomedical and Life Sciences*, *1055–1056*, 119–124.

Ma, W., Yang, L., Lv, Y., Fu, J., Zhang, Y., & He, L. (2017). Determine equilibrium dissociation constant of drug-membrane receptor affinity using the cell membrane chromatography relative standard method. *Journal of Chromatography. A*, *1503*, 12–20.

Nie, J., Li, Q., Wu, J., Zhao, C., Hao, H., Liu, H., … Wang, Y. (2020). Establishment and validation of a pseudovirus neutralization assay for SARS-CoV-2. *Emerging Microbes & Infections*, *9*(1), 680–686.

Pant, S., Singh, M., Ravichandiran, V., Murty, U. S. N., & Srivastava, H. K. (2020). Peptide-like and small-molecule inhibitors against Covid-19. *Journal of Biomolecular Structure and Dynamics*, *6*, 1–10.

Skarstein Kolberg, E. (2020). ACE2, COVID19 and serum ACE as a possible biomarker to predict severity of disease. *Journal of Clinical Virology*, *126*, 104350.

Tahir Ul Qamar, M., Alqahtani, S. M., Alamri, M. A., & Chen, L. L. (2020). Structural basis of SARS-CoV-2 3CLpro and anti-COVID-19 drug discovery from medicinal plants. *Journal of Pharmaceutical Analysis*, *10*(4), 313–319.

Towler, P., Staker, B., Prasad, S. G., Menon, S., Tang, J., Parsons, T., … Pantoliano, M. W. (2004). ACE2 X-ray structures reveal a large hinge-bending motion important for inhibitor binding and catalysis. *Journal of Biological Chemistry*, *279*(17), 17996–18007.

Tsai, C. C., Lin, C. S., Hsu, C. R., Chang, C.-M., Chang, I.-W., Lin, L.-W., … Wang, J.-L. (2018). Using the Chinese herb *Scutellaria barbata* against extensively drug-resistant *Acinetobacter baumannii* infections: in vitro and in vivo studies. *BMC Complementary and Alternative Medicine*, *18*(1), 96.

Wang, Z., & Babina, M. (2020). MRGPRX2 signals its importance in cutaneous mast cell biology: Does MRGPRX2 connect mast cells and atopic dermatitis? *Experimental Dermatology*, *29*(11), 1104–1111.

Wang, M., Cao, R., Zhang, L., Yang, X., Liu, J., Xu, M., … Xiao, G. (2020). Remdesivir and chloroquine effectively inhibit the recently emerged novel coronavirus (2019-nCoV) in vitro. *Cell Research*, *30*, 269–271.

Wu, X., Zhi, F., Lun, W., Deng, Q., & Zhang, W. (2018). Baicalin inhibits PDGF-BB-induced hepatic stellate cell proliferation, apoptosis, invasion, migration and activation via the miR-3595/ACSL4 axis. *International Journal of Molecular Medicine*, *41*(4), 1992–2002.

Xiong, X., Wang, P., Su, K., Cho, W. C., & Xing, Y. (2020). Chinese herbal medicine for coronavirus disease 2019: A systematic review and meta-analysis. *Pharmacological Research*, *160*, 105056.

Yan, R., Zhang, Y., Yaning, L., Lu, X., Guo, Y., & Zhou, Q. (2020). Structural basis for the recognition of SARS-CoV-2 by full-length human ACE2. *Science*, *367*(6485), 1444–1448.

Yang, T., Shi, X., Kang, Y., Zhu, M., Fan, M., Zhang, D., & Zhang, Y. (2018). Novel compounds TAD-1822-7-F2 and F5 inhibited HeLa cells growth through the JAK/Stat signaling pathway. *Biomedicine & Pharmacotherapy*, *103*, 118–126.

Yang, X. X., Wang, Y. W., Zhang, X. X., Chang, R., & Li, X. (2011). Screening vasoconstriction inhibitors from traditional Chinese medicines using a vascular smooth muscle/cell membrane chromatography-offline-liquid chromatography-mass spectrometry. *Journal of Separation Science*, *34*(19), 2586–2593.

Zhang, T., Ding, Y. Y., An, H. L., Feng, L., & Wang, S. (2015). Screening anti-tumor compounds from *Ligusticum wallichii* using cell membrane chromatography combined with high-performance liquid chromatography and mass spectrometry. *Journal of Separation Science*, *38*(18), 3247–3253.

Zhao, Q., Chen, X. Y., & Martin, C. (2016). Scutellaria baicalensis, the golden herb from the garden of Chinese medicinal plants. *Science Bulletin (Beijing)*, *61*(18), 1391–1398.

Zhong, L. L. D., Lam, W. C., Yang, W., Chan, K. W., Sze, S. C. W., Miao, J., … Wong, V. T. (2020). Potential targets for treatment of coronavirus disease 2019 (COVID-19): A review of Qing-Fei-Pai-Du-Tang and its major herbs. *The American Journal of Chinese Medicine*, *48*(5), 1051–1071.

Zhong, Z., Sanchez-Lopez, E., & Karin, M. (2016). Autophagy, inflammation, and immunity: A troika governing cancer and its treatment. *Cell*, *166*(2), 288–298.

Zhou, P., Yang, X. L., Wang, X. G., Hu, B., Zhang, L., Zhang, W., … Shi, Z.-L. (2020). A pneumonia outbreak associated with a new coronavirus of probable bat origin. *Nature*, *579*(7798), 270–273.

How to cite this article: Gao J, Ding Y, Wang Y, Liang P, Zhang L, Liu R. Oroxylin A is a severe acute respiratory syndrome coronavirus 2-spiked pseudotyped virus blocker obtained from Radix Scutellariae using angiotensin-converting enzyme II/cell membrane chromatography. *Phytotherapy Research*. 2021;35:3194–3204. https://doi.org/10.1002/ptr.7030